

Terahertz-wave generation in quasi-phase-matched GaAs

K. L. Vodopyanov^{a)} and M. M. Fejer

Edward L. Ginzton Laboratory, Stanford University, Stanford, California 94305

X. Yu and J. S. Harris

Solid State Photonics Laboratory, Stanford University, Stanford, California 94305

Y.-S. Lee and W. C. Hurlbut

Department of Physics, Oregon State University, Corvallis, Oregon 97331

V. G. Kozlov

Microtech Instruments, Inc., Eugene, Oregon 97403

D. Bliss and C. Lynch

Hanscom Air Force Research Laboratory, Bedford, Massachusetts 01731

(Received 17 June 2006; accepted 4 August 2006; published online 4 October 2006)

The authors demonstrate an efficient room temperature source of terahertz radiation using femtosecond laser pulses as a pump and GaAs structures with periodically inverted crystalline orientation, such as diffusion-bonded stacked GaAs and epitaxially grown orientation-patterned GaAs, as a nonlinear optical medium. By changing the GaAs orientation-reversal period (504–1277 μm), or the pump wavelength (2–4.4 μm), we were able to generate narrow-bandwidth (~ 100 GHz) terahertz wave packets, tunable between 0.9 and 3 THz, with the optical-to-terahertz photon conversion efficiency of 3.3%. © 2006 American Institute of Physics.

[DOI: 10.1063/1.2357551]

In the optical rectification (OR) process, terahertz output is produced in an electro-optic medium via self-difference-frequency mixing between Fourier components of the optical pulse. First demonstrated with picosecond pulses in LiNbO_3 ,^{1,2} ZnTe , ZnSe , CdS , and quartz¹ crystals, this technique was later extended to femtosecond pulses³ and became an established way of generating single-cycle broadband terahertz radiation. Typically, thin (~ 1 mm or less) electro-optic crystals are used because of phase matching constraints as well as high absorption in conventional crystals (LiNbO_3 and ZnTe) at terahertz frequencies. Optical-to-terahertz conversion efficiencies achieved so far by optical rectification methods are low, typically 10^{-6} – 10^{-9} .⁴ Recently, conversion efficiency of 5×10^{-4} was reported.⁵ The authors used optical rectification in LiNbO_3 , in a noncollinear geometry, with 150 fs 300–500 μJ optical pump pulses at 800 nm with a tilted intensity front. Lee *et al.*⁶ demonstrated that in a quasi-phase-matched (QPM) structure, the interaction length between terahertz and optical pulses can be dramatically extended; terahertz output in this case is produced in the form of narrow-band wave packets. With 200 fs pulses at 800 nm and periodically poled lithium niobate crystal, cryogenically cooled (18 K) to reduce terahertz absorption, the authors achieved 10^{-5} conversion efficiency.⁷

Zinc blende semiconductors (GaAs and GaP) show great potential for QPM terahertz generation because of their small, as compared to lithium niobate, terahertz absorption coefficient α_{THz} [in GaAs, for example, $\alpha_{\text{THz}} = 0.5$ – 4.5 cm^{-1} at 1–3 THz (Ref. 8)], small mismatch between the optical group and terahertz phase velocities, and high thermal conductivity. Terahertz-wave generation was demonstrated recently in QPM GaAs using optical rectification of femtosecond pulses⁹ and in QPM GaP using differ-

ence frequency generation (DFG) with nanosecond pulses.¹⁰ In this letter, we report on an efficient widely tunable source of terahertz radiation based on OR in quasi-phase-matched GaAs structures.

In our experiment, tunable pump pulses centered at 2–4.4 μm were produced using a parametric amplifier (OPerA, Coherent Inc.) system pumped by 800 nm Ti:sapphire pulses after a regenerative amplifier (Legend, Coherent Inc.). To achieve $\lambda > 3$ μm wavelengths, an additional difference frequency generation stage was used. Typical pulse durations were ~ 100 fs, repetition rate 1 kHz, and pulse energy up to 3 μJ . The > 2 μm pump wavelength range was chosen to avoid two-photon absorption (2PA) in GaAs (2PA edge at 1.74 μm), which creates additional losses both at pump wavelength and at terahertz frequencies (in the latter case because of induced absorption due to generated free carriers).

We have used two types of QPM GaAs samples: (i) diffusion-bonded GaAs (DB-GaAs) produced by stacking and bonding together alternately rotated $\langle 110 \rangle$ GaAs plates;¹¹ wafer fusion in this case creates a monolithic body with periodic change in the nonlinear coefficient, and (ii) orientation-patterned GaAs (OP-GaAs) grown by a combination of molecular beam epitaxy (MBE), photolithography, and hydride vapor phase epitaxy (HVPE),¹² where periodic inversions of the crystallographic orientation are grown into the material. While DB-GaAs provides larger apertures, OP-GaAs has more reproducible technology and allows lithographic definition of QPM gratings. The samples were not anti-reflection coated and their main parameters are listed in Table I.

The optical pump beam with a beam size ($1/e^2$ intensity radius) ranging between $w = 300$ μm and 1.5 mm propagated along the $\langle 110 \rangle$ direction of GaAs. A Picarin lens was used to collect the terahertz radiation to the liquid-He-cooled silicon

^{a)}Electronic mail: vodopyan@stanford.edu

TABLE I. Parameters of the QPM GaAs samples.

Sample	QPM type	Aperture (mm ²)	Length (mm)	QPM period (μm)
DB-77	DB-GaAs	10 \times 10	6	504
A3	OP-GaAs	0.4 \times 3	3	1277
A10	OP-GaAs	0.4 \times 3	10	1277
B5	OP-GaAs	0.4 \times 3	5	759
B10	OP-GaAs	0.4 \times 3	10	759
C5	OP-GaAs	0.4 \times 3	5	564

bolometer which measured the average power of terahertz pulses. A black polyethylene filter was used to block optical radiation. To measure the spectral properties of terahertz radiation (Fig. 1), we have used a Michelson interferometer, composed of two 2-in.-diameter flat gold mirrors and a 25- μm -thick Mylar beam splitter.

Theoretically, the frequency of terahertz radiation produced by the QPM optical rectification is centered⁶ at $\nu_{\text{THz}} = c/\Lambda\Delta n$, corresponding to the zero wave-vector mismatch condition; c is the speed of light, $\Delta n = n_{\text{THz}} - n_{\text{opt}}^{\text{gr}}$ is the mismatch between the terahertz refractive index and the optical group refractive index, and Λ is the QPM period. For GaAs, n_{THz} is nearly constant⁸ ≈ 3.6 at frequencies well below the lowest phonon resonance¹³ (8.1 THz) and $n_{\text{opt}}^{\text{gr}}$ varies¹⁴ between 3.43 ($\lambda = 2 \mu\text{m}$) and 3.33 ($4.4 \mu\text{m}$). The spectral width of terahertz wave packets is determined by the QPM acceptance bandwidth $\Delta\nu_{\text{THz}} = c/L\Delta n$, where L is the length of the crystal.

The power spectra of terahertz pulses were extracted in our experiment by computing the amplitudes of the Fourier transforms of Michelson interferograms. Figure 2 shows both original interferograms and computed spectra for different samples and different pump wavelengths. The spectra were noticeably distorted by water vapor absorption (also shown in Fig. 2). Interestingly, for sample A10 with the largest QPM period, 1277 μm , we observed [Fig. 2(d)] a second peak at ~ 2.6 THz which is likely to be the third order QPM peak, at approximately three times the frequency of the main peak. The amplitudes of both peaks are comparable: efficiency reduction ($1/3^2$) due to the third order QPM is offset by the ν_{THz}^2 factor which appears in the expression for the efficiency of any DFG-like process.¹⁵

Experimentally observed central frequencies and bandwidths of terahertz pulses are in good agreement with theoretical predictions based on known GaAs dispersion relations.^{8,14} By changing the pump wavelength or GaAs QPM period, we generated terahertz wave packets with cen-

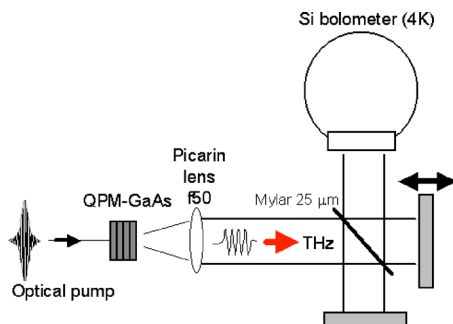


FIG. 1. (Color online) Experimental setup for terahertz generation and Michelson interferometry.

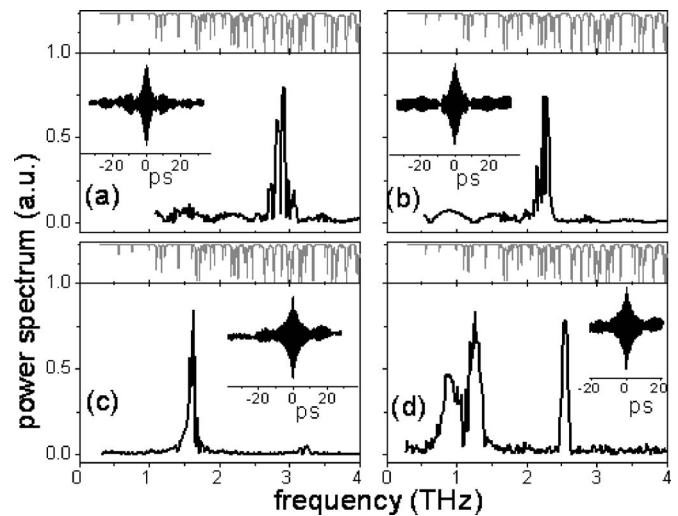


FIG. 2. Spectra of terahertz pulses obtained by Michelson interferometry. (a) Sample DB-77, pump at $2.03 \mu\text{m}$; (b) sample DB-77, pump at $3.5 \mu\text{m}$; (c) sample B10, pump at $4.4 \mu\text{m}$; and (d) sample A10, pump at $4.4 \mu\text{m}$. The spectra are distorted by water vapor absorption (high-resolution transmission molecular absorption database water transmission spectrum for 10 cm path is shown on top of each plot). Insets show original interferograms.

tral frequencies between 0.9 and 3 THz. The tuning curve for the $4.4 \mu\text{m}$ optical pump is shown in Fig. 3.

We found that the terahertz beam propagated collinearly with respect to the optical pump and was close to diffraction limited (a pinhole method was used to measure the far-field terahertz beam size). Figure 4 shows optical-to-terahertz conversion efficiency η_{THz} as a function of peak pump intensity I_0 inside the sample (DB-77, pump at $\lambda = 3.5\text{--}4.4 \mu\text{m}$). The pump beam size varied in this case between 810 μm (open circles), 520 μm (closed circles), and 300 μm (crossed circles). One can see that the linear dependence of η_{THz} , expected by theory, rolls off for $I_0 > 2 \text{ GW}/\text{cm}^2$. This roll-off behavior was also observed at similar intensities at shorter, $\lambda \sim 2 \mu\text{m}$ pump. The onset of saturation is most likely due to nonlinear refraction (n_2) in GaAs which induces self-phase modulation and self-focusing of the optical pulses. Indeed, we have measured $n_2^I \approx 1.5 \times 10^{-4} \text{ cm}^2/\text{GW}$ for GaAs at $3.5 \mu\text{m}$ and estimated that at $I_0 = 2 \text{ GW}/\text{cm}^2$ and $L(\text{GaAs}) = 6 \text{ mm}$, the nonlinear phase shift at beam center reaches $\sim \pi$.

Terahertz conversion efficiencies for OP-GaAs samples A3 (also shown on Fig. 4) and B5 are very similar to each other and are smaller, by a factor of ~ 3.5 , than that of the DB-77 sample (in both cases the pump was at $3.5 \mu\text{m}$, cen-

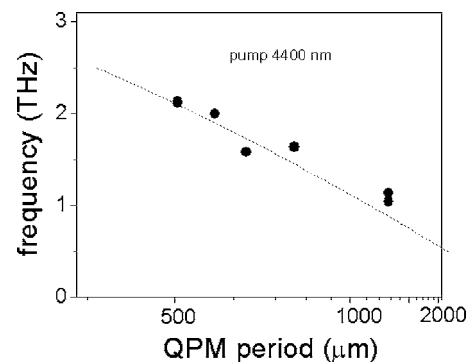


FIG. 3. Terahertz tuning curve for the $4.4 \mu\text{m}$ pump wavelength. Dashed curve—theoretical.

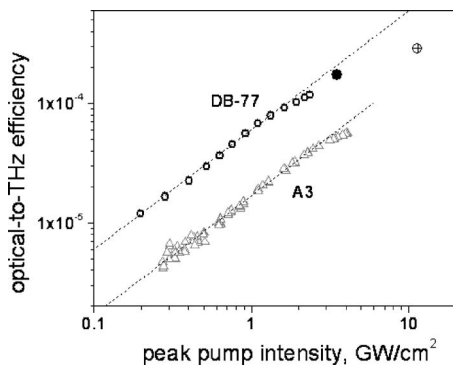


FIG. 4. Optical-to-terahertz conversion efficiency as a function of peak pump intensity for samples DB-77 (central frequency ~ 2.2 THz, circles) and A3 (central frequency ~ 1.5 THz, triangles). The average pump beam sizes were $810 \mu\text{m}$ (open circles), $520 \mu\text{m}$ (closed circles), $590 \mu\text{m}$ (triangles), and $300 \mu\text{m}$ (crossed circles). The pump wavelengths were $3.5 \mu\text{m}$ (open circles and triangles) and $4.4 \mu\text{m}$ (filled and crossed circles). Dashed lines—linear fits.

tral frequencies at 1.5 and 1.76 THz, correspondingly). We attribute smaller terahertz outputs in A3 and B5 to the beam clipping: their limiting dimension (height) is only 0.4 mm , comparable to terahertz wavelengths ($\sim 200 \mu\text{m}$). Also, for the DB-77 sample, pump polarization was aligned along $\langle 111 \rangle$, while for A3 and B5 it was along $\langle 110 \rangle$; in the former case, the nonlinear optical coefficient was larger: $\sqrt{4/3}d_{14}$ vs d_{14} .

In the DB-77 sample, we generated 0.66 nJ of output at 2.2 THz , with $2.3 \mu\text{J}$ of pump pulse energy ($w=300 \mu\text{m}$), which corresponds to optical-to-terahertz conversion efficiency of 2.9×10^{-4} , internal efficiency of 8.7×10^{-4} (the samples were uncoated), and photon conversion efficiency of 1.1% (internal photon efficiency of 3.3%). These efficiencies are in accord with the calculated values,¹⁵ based on the known nonlinear optical coefficient for optical rectification $d_{\text{eff}}=2/\pi \times d_{14}=2/\pi \times 47 \text{ pm/V}$, derived from the electro-optical coefficient $r_{14}(\text{GaAs})=1.5 \text{ pm/V}$.¹⁶ We note that the measured conversion efficiency can be affected by water va-

por absorption along the beam path ($\sim 30 \text{ cm}$).

In conclusion, we demonstrated efficient terahertz generation with 3.3% internal photon efficiency and with only $2.3 \mu\text{J}$ of pump pulse energy. The limit for efficiency was set by parasitic $\chi^{(3)}$ -effects that can be avoided¹⁵ by using DFG with longer (picosecond) pulses. Thus, periodic GaAs structures show promise for optical terahertz generation in terms of robustness, wide tuning range, high conversion efficiency, and potential for scalability of the terahertz output power. Such source of terahertz radiation might be suitable for many applications including terahertz imaging and spectroscopy.

This work was sponsored by DARPA under AFOSR Grant No. FA9550-04-1-046.

¹T. Yajima and N. Takeuchi, *Jpn. J. Appl. Phys.* **9**, 1361 (1970).

²K. H. Yang, P. L. Richards, and Y. R. Shen, *Appl. Phys. Lett.* **19**, 320 (1971).

³L. Xu, X.-C. Zhang, and D. H. Auston, *Appl. Phys. Lett.* **61**, 1784 (1992).

⁴Peter H. Siegel, *IEEE Trans. Microwave Theory Tech.* **50**, 910 (2002).

⁵A. G. Stepanov, J. Kuhl, I. Z. Kozma, E. Riedle, G. Almási, and J. Hebling, *Opt. Express* **13**, 5762 (2005).

⁶Y.-S. Lee, T. Meade, V. Perlin, H. Winful, T. B. Norris, and A. Galvanauskas, *Appl. Phys. Lett.* **76**, 2505 (2000).

⁷Y.-S. Lee, T. Meade, M. DeCamp, T. B. Norris, and A. Galvanauskas, *Appl. Phys. Lett.* **77**, 1244 (2000).

⁸R. H. Stolen, *Appl. Phys. Lett.* **15**, 74 (1969).

⁹K. L. Vodopyanov, M. M. Fejer, D. M. Simanovskii, V. G. Kozlov, and Y.-S. Lee, *Conference on Lasers and Electro-Optics, Technical Digest, Baltimore, MD, May 2005* (Optical Society of America, Washington, DC, 2005), Paper No. CWMI.

¹⁰I. Tomita, H. Suzuki, H. Ito, H. Takenouchi, K. Ajito, R. Rungsaawang, and Y. Ueno, *Appl. Phys. Lett.* **88**, 071118 (2006).

¹¹L. A. Gordon, G. L. Woods, R. C. Eckardt, R. K. Route, R. S. Feigelson, M. M. Fejer, and R. L. Byer, *Electron. Lett.* **29**, 1942 (1993).

¹²L. A. Eyres, P. J. Tourreau, T. J. Pinguet, C. B. Ebert, J. S. Harris, M. M. Fejer, L. Becouarn, B. Gerard, and E. Lallier, *Appl. Phys. Lett.* **79**, 904 (2001).

¹³W. J. Moore and R. T. Holm, *J. Appl. Phys.* **80**, 6939 (1996).

¹⁴T. Skauli, P. S. Kuo, K. L. Vodopyanov, T. J. Pinguet, O. Levi, L. A. Eyres, J. S. Harris, and M. M. Fejer, *J. Appl. Phys.* **94**, 6447 (2003).

¹⁵K. L. Vodopyanov, *Opt. Express* **14**, 2263 (2006).

¹⁶D. N. Nikogosyan, *Properties of Optical and Laser-Related Materials* (Wiley, Chichester, 1997), p. 333.